Please cite the Published Version

Insights into the electrochemical behaviour of brominated RNA nucleobases at microband screen-printed graphite electrodes

Ana Casanova [a,*], Alicia Gomis-Berenguer [b], Craig E Banks [c], Jesus Iniesta [b,d,*]

[a] CNRS, ICMN UMR 7374, Universit´e d'Orl´eans, Orl´eans Cedex 2, 45071, France
[b] Institute of Electrochemistry, University of Alicante, Alicante, Spain
[c] Faculty of Science and Engineering, Manchester Metropolitan University, Dalton Building, Chester Street, Manchester M1 5GD, United Kingdom
[d] Physical Chemistry Department, University of Alicante, Alicante, Spain

Nucleobases are nitrogenous compounds that form nucleotides, the building blocks of DNA and RNA. Modification of DNA and RNA through various epigenetic mechanisms can occur at different levels and plays a fundamental role in several biological processes; these modifications are significantly correlated with a variety of diseases related to changes in gene function and expression alterations. Different types of epigenetic modifications of nucleobases such as methylation, oxidation, and halogenation can occur, so interest in the rapid and simple techniques for detecting of these DNA and RNA nucleobase modifications has been growing in the recent decades. Hence, the aim of the research is to provide a useful tool to detect diseases or cellular dysfunctions at an early stage. This work will deal with the use of miniaturized electrochemical sensors for the detection of epigenetic modifications in nucleobases. For this purpose, the electrochemical response of graphite screen-printed platforms in two geometric configurations - disc and microband - was explored for the quantitative and qualitative determination of brominated nucleobases. A comprehensive analysis of the electrochemical behavior of the halogenated and non-halogenated nucleobases was carried out, focusing on the effect on the geometry of the working electrode. At last, an identification of brominated nucleobases in synthetic mixed solutions was performed.

1. Introduction

Nucleobases, as the simplest entities of nucleic acids and nucleosides, are biological compounds, which are the components of nucleotides, which together form the basic building blocks of DNA. Among the nucleobases, adenine (A), guanine (G), cytosine (C) and thymine (T) are found in DNA, while adenine, guanine, cytosine and uracil (U) are present in RNA. The nucleobases of DNA or RNA are subject to continuous external attack or invasions by parasitic agents that can have consequences in the production of chronic inflammation [1,2]. In this regard, covalent modification of DNA through various epigenetic mechanisms plays an important role in several biological processes in the human body, triggering the deviation of normal physiological functions and prone to, among others, aging-related diseases, neurodegenerative diseases and cancer, and increasing the risk of death. Similarly, cellular RNA can also undergo these alterations, with a chemically modified structure, thus affecting RNA metabolism. An example of this refers to the addition of the methyl group at C5 position of C as one of the most common modifications in CpG islands (area with a high frequency of CpG dinucleotides), as well as the methylation of G at C7 position. The hypermethylation or aberrant methylation of CpG islands are linked to suppressor genes or transcriptional silencing [2] with consequences in the occurrence of various human malignancies and cancer diseases [3,4].

The modification of DNA or RNA nucleobases is also related on what kind of chemical agent is involved, i.e., nitric oxide (NOx), hypochlorous acid (HClO), hypobromous acid (HBrO) or hydrogen peroxide (H_2O_2), and their dosage concentration. In carcinogenesis, leukocyte-derived peroxidases, myeloperoxidase (MPO) and eosinophil peroxidase (EPO), utilize H_2O_2 and halides (Cl- and Br-) present in plasma leading to the formation of halogenated products by reacting nucleobases with the generated oxidizing agents (HOCl and HOBr). These epigenetic modifications cause DNA damage at the site of inflammation through chlorination and bromination of bioactive species, such as 5-chlorocytosine

---

and 5-bromocytosine, respectively [5].

Concerning bromination in particular, studies on the effect of C8-bromination on G and A have been performed by determining the absorption and fluorescence spectra in oxygenated and UV-irradiated aqueous solutions [6]. The incorporation of 8-bromoguanine (BrG) instead of G into DNA may have consequences on the stabilization of the Z-form of the polymeric pattern of the double-stranded DNA macromolecule, but may also trigger on the appearance of dysfunction disorders or diseases [7]. Despite the fact that the excessive presence of BrG results to be involved in inflammation events inducing a G → T mutation but also G → C, G → A among others, covalent modification can be repaired by the participation of glycosylates acting in the repair of BrG mispairs [8]. In addition, and beyond G modification, bromination of U and A at C8 position served as radiosensitizers in human cells to increase the sensitivity to radiation damage caused by ultraviolet light and low energy electrons [9]. As for the RNA nucleobase, bromination of U (BrU) has been found to induce transition mutations by mispairing with G during replication, and it is still uncertain whether the bulky bromine atom in BrU dictates the stacking or self-association of DNA bases [10].

The rapid and easy detection of RNA nucleobases modifications has attracted increasing interest in recent decades as a useful tool for an early detection of diseases. The presence of nucleosides in urinary samples has been studied by Struck et al. [11] using chromatographic techniques (reversed-phase UPLC, hydrophilic interaction chromatography) coupled with different conventional detectors such as UV or mass spectrometry. A highly sensitive ELISA technique is a common immunoassay tool for the determination of epigenetic modification in nucleosides and this was evidenced by the determination of methylation in cytidine, adenosine, uridine or guanosine [12]. Other epigenetic modification in C, 5-hydroxymethylcytosine, has been determined by different techniques, such as single-molecule imaging methods, with high sensitivity in early stage of cancer disease with few nanograms per milliliter of plasma, which pursues the detection of single molecule epigenetic technology [13,14]. In this regard, electrochemical tools have great potential to fulfil this need in the field of point-of-care methods using electrochemical devices capable of detecting methylation and hydroxymethylation in C [15−18]. However, to the best of the authors knowledge, there are no fundamental studies on the electroanalysis or electrochemical response of brominated nucleic bases and their derivates, nor on the use of electrochemical techniques for the sensing of brominated nucleosides on DNA. The electrochemistry of 5-chlorocytosine (ClC), as halogenated nucleobase, was reported solely by Sanjuan et al., and the electrochemical oxidation of 5-bromocytosine (BrC) was given only for comparative purposes [19].

In a point of thriving interest, this manuscript therefore aims to explore the electrochemical response of brominated C, U, A and G and their unmodified counterparts (Scheme 1) since their electrochemistry remains almost unknown. Two different geometrical configurations (disc and microband) of graphite screen-printed electrodes have been explored in an attempt to study the electrochemical behaviour and present electroanalytical figures of merit towards the sensing of brominated nucleobases.

2. Materials and methods

Chemicals and reagents. Nucleobases (cytosine, C, uracil, U, adenine, A, guanine, G, 5-bromouracyl, BrU, 8-bromoadenine, BrA, and 8-bromoguanina, BrG) were purchased from Sigma Aldrich with 99.9 % purity and used without further purification. The synthesis of 5-bromocytosine (BrC, <95 % plus purity) was performed by following the synthesis process described in reference [19], and purity was evaluated by ^{1}H NMR spectroscopy.

Solutions of the different nucleobases were prepared in 0.1 M phosphate buffer solution (PBS) at pH 7.0 (close to physiologic pH), unless other pH is indicated. Saturated solutions of G and BrA were prepared and then filtered through a 45 μm pore size nylon filter (Millipore MILLEX-HN) in order to remove excess insoluble base. The final concentrations were determined by ultraviolet spectroscopy at 243 nm and 260 nm, and molar absorptivities of 10,700 M^{-1} cm^{-1} and 15,200 M^{-1} cm^{-1} were taken for G and BrA, respectively [20]. All solutions were prepared with deionised water of resistivity not <18.2 MΩ cm.

Electrochemical experiments: Cyclic voltammetry (CV) and square wave voltammetry (SWV) were used to explore the electrochemical response of the distinct nucleobases on the screen-printed platforms. The scan rate applied for CV was 20 mV/s and the SWV parameters employed in all experiments were as follows: pulse amplitude, 50 mV; potential step, 2 mV; frequency 4 Hz. All of the above SWV parameters were the optimal values in terms of current intensity for the electrooxidation of the brominated nucleobases. Screen-printed graphite electrodes (SPGEs) were fabricated at Manchester Metropolitan University, with appropriate stencil designs using a microDEK 1760RS screen-printing machine. Commercially available carbon-graphite ink (Gwent Electronic Materials Ltd., UK) was screen-printed onto a flexible polyester film; then, after curing step, Ag/AgCl paste was screen-printed to define the reference electrode. Finally, a dielectric paste ink was printed to cover the connections. Concerning the geometry of the working
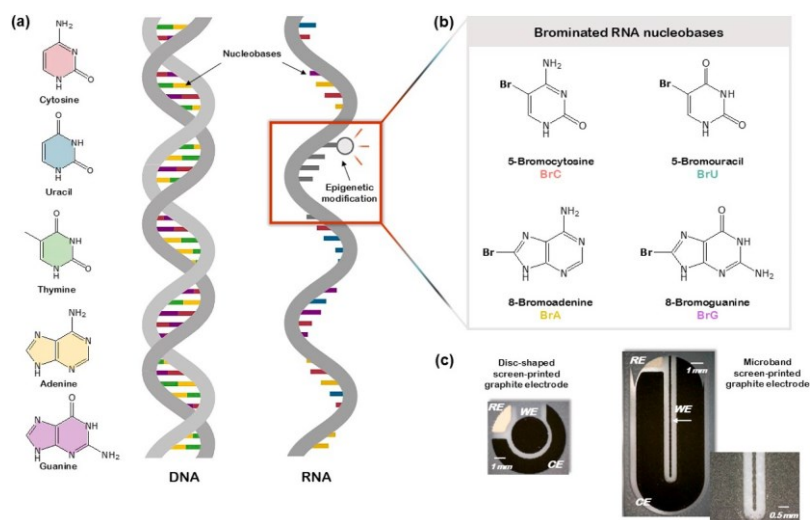
Scheme 1. Schematic representation of (a) DNA and RNA nucleobases, (b) brominated epigenetic modifications in RNA nucleobases, (c) disc-shaped and microband screen-printed graphite electrodes.

electrode, two working electrode configurations were employed: disc-shaped electrode with a diameter of 3.1 mm (dSPGE) and microband-shaped electrode with dimensions of 0.1 × 10 mm (mbSPGE) [21].

Voltammetric measurements were performed using a Bio-Logic potentiostat (VMP-300). CV and SWV measurements were referred to the reference electrode. All electrodes were conditioned prior to use by cyclic voltammetry, consisting of a sweep between 0 and +1.4 V of six scans in a 0.1 M phosphate buffer solution at pH 7.0.

3. Results and discussions

3.1. Electrochemical behaviour of nuceleobases and brominated nucleobases on dSPGE

The effect of the Br- covalent modification of nucleobases on the electrochemical response at disc-shaped screen-printed graphite electrodes (dSPGE, geometrical area 7.55 mm^2) in 0.1 M PBS pH 7.0 is described in Figure S1. In the same figure, the cyclic voltammetry profiles of the studied unmodified nucleobases, C, U, A, and, G are shown, and their irreversible oxidation thorough their nitrogenous group was evidenced at peak potentials of +1.20, +1.18, +0.98, and +0.58 V vs. Ag/AgCl, respectively, which is in agreement with previous results reported in the literature using carbon-based electrodes [22,23]. For all the CV experiments, a slight general decrease of the current intensity signal was observed for second scan being quite stable after at least 10 sucessive scans, this behaviour is ascribed to the adsorption of oxidation products on the electrode surface, as described in the literature for the carbon-based electrodes [24,25]. The peak potentials for the electro-oxidation of brominated nucleic bases (BrC, BrU, and BrA) shifted to more negative potentials (Figure S1 and 1), ca. 100 mV, related to the sligh electron withdrawing of bromine group. Nevertheless, the exception to the above behaviour occurs for the electrochemical response of BrG, where oxidation peak potentials of G and BrG appear close to each other.

Fig. 1 depicts a more detailed electroanalysis of the brominated nucleobases and their unmodified counterparts carried out by SWV when a potential excursion was performed from 0 to +1.60 V vs. Ag/AgCl. At 0.5 mM of the pyrimidine bases (C and U), the potential peak associated with their electrooxidation showed a fully anodic wave in the potential range between +1.00 and +1.40 V vs. Ag/AgCl, exhibiting peak potentials closer to +1.25 and +1.20 V vs. Ag/AgCl for C and U, respectively. In contrast, purine bases, G and A, at 0.04 mM and 0.2 mM, respectively, were oxidised at low positive potentials, where G is the easiest to oxidise (+0.60 and +0.86 V vs. Ag/AgCl for G and A, respectively). Generally, the fact that G is the most easily oxidized nucleobase is well known, being the main target of oxidizing species [26, 27].

In parallel with the behaviour observed by cyclic voltammetry, the SWV profiles of the brominated nucleobases presented a well-defined oxidation peak whose potential was shifted by about -100 mV for BrC and BrA, and approximately 300 mV for the BrU compared to the potential of the oxidative peak of their unmodified nucleobase (see Table 1). It should be noted that for A-BrA and G-BrG pairs, lower concentrations were shown for comparison purposes (0.2 mM of A and BrA, and 0.05 mM of G, 0.1 mM of BrG), due to solubility limitations of BrA and G in water. Overall, the lower oxidation potential of the brominated bases could be explained by the additional resonance stabilisation of the ring by the electron-withdrawing effect of the Br atom, as observed by Sanjuan et al. [19]. The SWV of G and BrG exhibited a main oxidation peak close to +0.60 V for both nucleobases (the lowest potential peak was found for the lowest concentration of BrG -0.1 mM-, Table 1), which was similar to previously reported in the literature [23, 28,29]. Notably, as observed in the cyclic voltammetry profiles (Figure S1), there was an additional anodic peak at +1.35 V and +1.20 V for G and BrG, respectively, which is presumably attributed to the oxidation of by-products formed during the electrooxidation of G and BrG at pH 7.0.

With respect to SWV current density, a rational comparison for the four nucleobases was challenging due to solubility limitations, so different bulk concentrations for brominated and non-brominated nucleobases needed to be considered. Nonetheless, and subsequent to background signal subtraction, comparison of the ratios of the current densities at peak potentials of brominated nucleobase over unmodified nucleobase (j_{Br}/j) for the same concentration revealed values of 0.66, 0.83, and 0.65 for C-BrC, U-BrU and A-BrA pairs, respectively, which denoted a different interaction of the brominated nucleobases with the surface of the dSPGE. Furthermore, as far as an intercomparison of the peak current densities of brominated nucleic bases at the same nominal
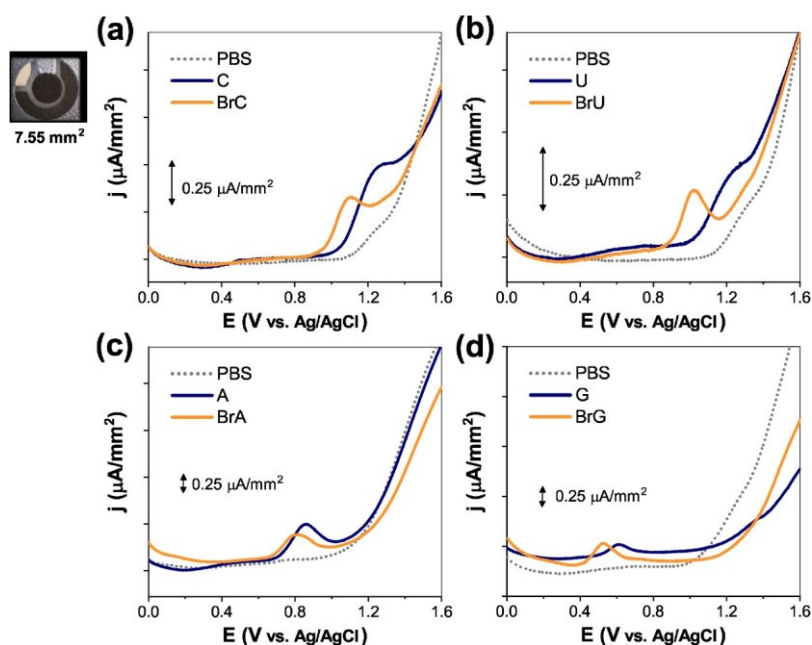

Fig. 1. Square wave voltammetry of brominated RNA nucleobases and their unmodified counterparts, in 0.1 M PBS pH 7.0 using a disc-shaped SPGE (0.5 mM for C, BrC, U and BrU, 0.04 mM for G, 0.09 mM for BrG, and 0.2 mM for A and BrA). SWV parameters: pulse amplitude, 50 mV; potential step, 2 mV; frequency 4 Hz.

Table 1
Peak potentials and current densities (after background subtraction) obtained for all brominated nucleobases and their unmodified counterparts using both SPGE platforms in 0.1 M PBS at pH 7.0.

Nucleobase	dSPGE		mbSPGE		Current density ratio j_{dSPGE}/j_{mbSPGE}
	Peak potential (V)	Current density (μA/mm²)	Peak potential (V)	Current density (μA/mm²)	
C (0.5 mM)	1.25 ± 0.02	0.4 ± 0.2	1.20 ± 0.02	2.5 ± 0.1	0.16
BrC (0.5 mM)	1.10 ± 0.05	0.27 ± 0.07	1.07 ± 0.01	1.98 ± 0.08	0.14
U (0.5 mM)	1.2 ± 0.1	0.2 ± 0.1	1.17 ± 0.02	2.21 ± 0.04	0.10
BrU (0.5 mM)	1.03 ± 0.02	0.20 ± 0.09	1.00 ± 0.02	1.7 ± 0.2	0.12
A (0.2 mM)	0.86 ± 0.04	0.63 ± 0.05	0.87 ± 0.02	1.3 ± 0.1	0.47
A (0.5 mM)	0.90 ± 0.03	0.87 ± 0.06	0.89 ± 0.01	1.4 ± 0.1	0.61
BrA (0.2 mM)	0.80 ± 0.02	0.41 ± 0.08	0.86 ± 0.01	0.83 ± 0.05	0.49
G (0.04 mM)	0.60 ± 0.03	0.18 ± 0.05	0.56 ± 0.02	0.40 ± 0.02	0.45
BrG (0.09 mM*;0.04 mM**)	0.54 ± 0.02*	0.22 ± 0.04*	0.50 ± 0.02**	0.37 ± 0.08**	–
BrG (0.5 mM)	0.60 ± 0.04	0.66 ± 0.08	0.59 ± 0.01	1.9 ± 0.1	0.35

concentration was concerned, the peak current density obtained from the SWV response of BrG was approximately twice that of BrU and BrC after background subtraction. However, the differences obtained in terms of peak current densities when comparing both brominated pu- rines and pyrimidines separately were less significant and may be mainly associated with the interaction between the nucleobase and the carbonaceous electrode.

3.2. Electrochemical behaviour as function of screen-printed electrode geometry

Fig. 2 shows the SWV profiles of the four pairs of nucleobases (non-halogenated and halogenated) under study obtained at the microband-shaped graphite screen-printed electrode (mbSPGE, geometric area of 1 mm²) in 0.1 M PBS at pH 7.0. Concerning the shape and electrode peak potential associated with the nucleic base oxidation, negligible differences were observed compared to the disc-shaped electrode (Fig. 2, Table 1), as was expected due to the same nature of the ink used for the preparation of the working electrode. The electrochemical system has the same actuators – graphite-based carbon ink and nucleobase – in both cases and, hence, the electrooxidation reaction was expected to occur in a similar manner.

By contrast, the size and geometry of the working electrode are well-known to have a major influence on the electrochemical behaviour in terms of variability in background charge currents and signal-to-noise ratio, or effect on the mass transport phenomena, which in turn leads to variability in the sensitivity of the electroanalytical measurements [30]. The length of the working electrode in this mbSPGE is on the macroscopic scale (10 mm), but in contrast, the width is significantly reduced down to microscale (0.1 mm), which presumably ensure the convergent diffusion that means increased mass transport resulting in greater current density compared with planar diffusion on dSPGE [21].

Accordingly, the effect of the working electrode geometry was studied through the redox probe $K_4Fe(CN)_6$ by CV over different scan rates (Figure S2). For dSPGE, a linear trend was achieved for Randles-Ševčík plot, j_p vs. square root of scan rate [31], in the range 5-500 mV/s obtaining a slope of 19.69 μA mm⁻² V⁻¹/² s¹/² (r^2 = 0.998) for anodic peak and -19.27 μA mm⁻² V⁻¹/² s¹/² (r^2 = 0.998) for cathodic peak, denoting a diffusion-controlled process. Nonetheless, the mbSPGE response was slightly out of the linear Randles-Ševčík equation at low scan rates (5 and 10 mV/s). This trend reflects a steady-state behaviour at low scan rates, while for above 10 mV/s the process reveals a control by reversible electron transfer process with anodic slopes of 34.31 and -36.36 μA mm⁻² V⁻¹/² s¹/² for anodic (r^2 = 0.992) and cathodic (r^2 = 0.999) peaks, respectively. This behaviour has been reported previously for this shape electrode, and is associated to the diffusion layer thickness over the microband electrode, which is larger than the smallest
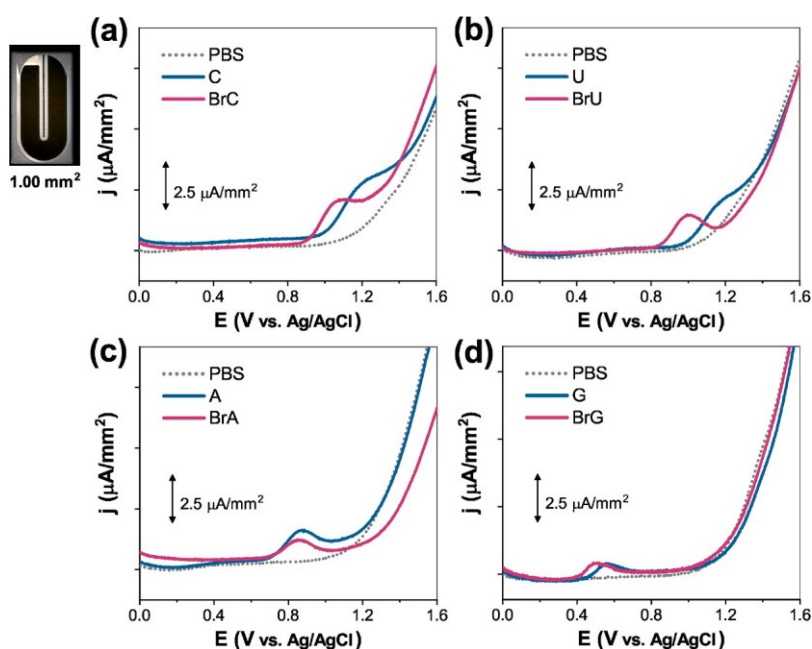

Fig. 2. Square wave voltammetry of brominated RNA nucleobases and their unmodified counterparts, in 0.1 M PBS pH 7.0 using a mbSPGE. SWV parameters: pulse amplitude, 50 mV; potential step, 2 mV; frequency 4 Hz.

electrode dimension at low scan rate, while the diffusion layer is reduced at higher scan rates [21].

From our results, the use of mbSPGE depicted a higher electroanalytical sensitivity enhanced by an increased mass transport (Fig. 2), overcoming the measured current density (low microampere range) on the dSPGE. The comparison of the current density ratios after background subtraction (j_{dSPGE}/j_{mbSPGE}) at the peak potentials of the disc-shaped SPGE and the microband-shaped SPGE at the same concentration for each nucleobase, as shown in Table 1, confirmed these trends. The j_{dSPGE}/j_{mbSPGE} values were found to be rather similar, between 0.10 and 0.16, for the pyrimidine bases (C and U); however, the ratios increased significantly for purine nucleic bases (A and G). This fact revealed that both the size and geometry of the working electrode do have a strong impact on the electrochemical performance of these screen-printed graphite electrodes, which is probably closely related to diffusion phenomena of the electroactive species present in the medium.

On the basis of the above experimental results, the microband electrode was selected to further investigate the electrochemical behaviour of the nucleobases and their corresponding halogenated homologues. As it was seen, the electrochemical performance with mbSPGE was optimal in terms of sensitivity compared to dSPGE, the improvement being directly related to the reduction of the geometrical area of the working electrode that in turn showed a higher current density under the same electroanalytical oxidation conditions.

3.3. Electroanalytical figures of merit

3.3.1. Effect of pH on the electrochemical response

The influence of buffer pH on the electrochemical responses of the nucleobases was investigated in the pH range from 5.5 to 8.0 upon mbSPGE at a fixed concentration (Fig. 3 and S3). Both the oxidation peak potentials and peak current densities were affected by the electrolyte pH, as general trend, when buffer pH increase, the oxidation peak potential is shifted towards more negative potential, indicating that protons were involved in the oxidation reaction mechanism (more rapidly deprotonation at higher pH). Observation of the SWV profiles obtained for A-BrA and G-BrG pairs reveals anodic humps at pH between 5.5 and 6.5 beyond +1.10 V vs. Ag/AgCl, which were more pronounced

for the brominated nucleobases (Figure S3).

The SWV were then analysed through a plot of peak potential over pH, as depicted in Fig. 3. First, for the unmodified nucleobases, a linear pH dependence has been found between the peak potentials of nucleic bases and the pH of the electrolyte with two well defined pH ranges 5.5−6.5 and 7.0−8.0. Accordingly, an inflexion point was observed between 6.5 and 7.0 for all the bases studied, being less pronounced for purine bases, A and G, which response is quasi linear in the whole pH range. This behaviour is probably related to the different acidity constants (pKa) of the nucleobases and, therefore, to the presence of a variety of tautomeric species present in each pH range [19,32]. The slopes of peak potential against pH obtained from the SWV responses at unmodified nucleic bases were found close to Nernstian behaviour (slope close to -59.16 mV), suggesting that the number of protons and electrons involved in the oxidation mechanism are equal. Regarding the brominated nucleobases, similar performance was observed for BrC and BrU following a near Nernstian behaviour in both pH ranges. Notwithstanding, brominated purines did not follow this trend, as changes in electrolyte pH provokes an abrupt decrease in the peak potential for the first pH range (5.5−6.5), followed by almost constant peak potential for the second range (7.0−8.0).

Due to the proximity of the physiological conditions and the simplicity of the electrochemical response, pH 7.0 was selected to carry on the electrochemical analysis over the concentration range of unmodified and brominated nucleobases.

3.3.2. Concentration range and calibration curves

To evaluate the analytical characteristics of the mbSPGE in the electro-oxidative detection of the non-halogenated and halogenated nucleobases, the calibration curves were constructed. Fig. 4 illustrates the current density obtained by SWV with increasing concentration of nucleic base. Overall, SWV responses of these molecules revealed a slight shift toward positive electrode potentials with the increase of concentration (below 50 mV) denoting irreversibility or partial adsorption (Figure S4).

The resulting calibration curve plots exhibited a linear relationship ($r^2 \geq 0.960$) for all brominated nucleobases. The concentration range was varied according to the solubility limit of the molecules studied,
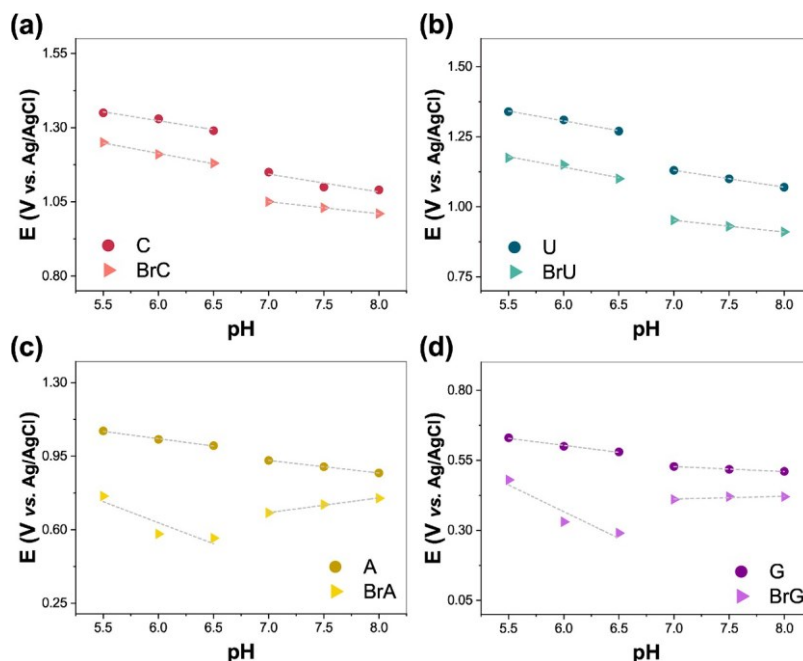

Fig. 3. Peak potential versus pH solution, obtained from the SWV response (parameters: pulse amplitude, 50 mV; potential step, 2 mV; frequency 4 Hz) after background subtraction, for (a) C-BrC, (b) U-BrU, (c) A-BrA, and (d) G-BrG pairs. The dash lines in the figure are guide for the eye.
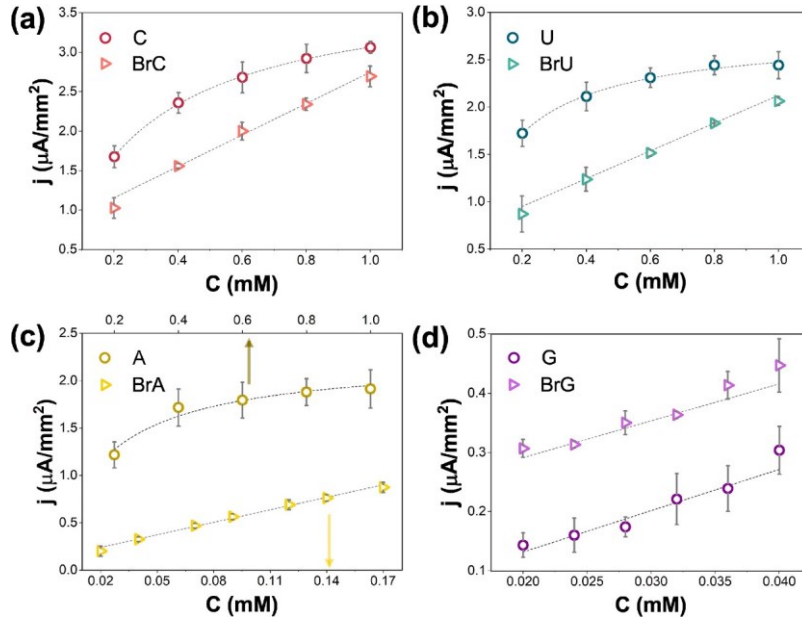
Fig. 4. Relationship between j_{peak} (after background subtraction) and nucleobase concentration obtained from SWV at mbSPGE in 0.1 M PBS at pH 7.0.

ranging from 0.2 to 1.0 mM, for BrC and BrU, while for BrA and BrG was from 0.02 to 0.17 mM, and from 0.02 to 0.04 mM, respectively. The reproducibility between electrodes was explored with three mbSPGEs (S/N = 3). The results indicated that this method enables the sensitive identification of brominated RNA nucleobases with high reproducibility (relative standard deviation, RSD, ≤ 5 %). The linear fitted equations of all brominated nucleobases are depicted in Eqs. (1)-4. A limit of detection (LOD) (S/N = 3) of 0.110, 0.111, 0.009, 0.003 mM was estimated for BrC, BrU, BrA, and BrG, respectively, applying the 3 Sd/m criteria, where *Sd* represents the standard deviation of the background signal and *m* is the slope of the calibration plot.

$$BrC : j_{peak} \left(\mu A / mm^2 \right) = 2.061 \cdot C_{BrC} (mM) + 0.687; r^2 = 0.990 \quad (1)$$

$$BrU : j_{peak} \left(\mu A / mm^2 \right) = 1.489 \cdot C_{BrU} (mM) + 0.610; r^2 = 0.995 \quad (2)$$

$$BrA : j_{peak} \left(\mu A / mm^2 \right) = 4.445 \cdot C_{BrA} (mM) + 0.142; r^2 = 0.993 \quad (3)$$

$$BrG : j_{peak} \left(\mu A / mm^2 \right) = 7.238 \cdot C_{BrG} (mM) + 0.148; r^2 = 0.960 \quad (4)$$

Conversely, different performance was observed for the unmodified nucleobases. Fig. 4 reveals that an adsorption and/or fouling phenomenon of mbSGE occurred and consequently, a non-linear response was found (with the exception of G). The results were fitted to the well-known Langmuir binding isotherms (Figure S5) which assumes there is an equilibrium between nucleobase and electrode surface, and is defined as $j = (j_{max} \bullet b \bullet C_i)/(1 + (b \bullet C_i))$; where C_i is the concentration of the nucleobase, j_{max} is the maximum peak current density, and b refers to adsorption energy [33]. The fitting of the electro-oxidation values of C, U and A to the Langmuir equation revealed b values of 3.87, 8.16, and 6.52 mM^{-1} for C, U and A, respectively (Eqs. (5), 6, and 7), indicating faster adsorption kinetics for U and A compared to the lower value obtained for C. These results indicate that the nucleobases C, U and A in the investigated concentration range were bound to the carbonaceous sur-

$$U : j_{peak} \left(\mu A / mm^2 \right) = \frac{22.63 \cdot C_i (mM)}{1 + 8.16 \cdot C_i (mM)}; r^2 = 0.993 \quad (6)$$

$$A : j_{peak} \left(\mu A / mm^2 \right) = \frac{14.67 \cdot C_i (mM)}{1 + 6.52 \cdot C_i (mM)}; r^2 = 0.947 \quad (7)$$

$$G : j_{peak} \left(\mu A / mm^2 \right) = 8.808 \cdot C_G (mM) + 0.038; r^2 = 0.949 \quad (8)$$

Presumably, the linear response of G (Eq. (8)) was associated with the narrow concentration studied (0.02−0.04 mM) in contrast to the wider concentration range tested for the rest of the nucleic bases (0.2−1.0 mM). It is worth noting that the main objective of this work was not the optimization of the sensing process for the nucleobases, hence lower concentration values were not tested in an attempt to exhaustively study the linear range, but relatively high concentrations (at the mM range) were used with the aim of analyzing the electrochemical performance of the nucleobases investigated.

In this sense, the presence of the Br functional group in the nucleobases influenced the oxidation process, as was clearly demonstrated by face electrode prior to their oxidation, as suggested by the Langmuir adsorption model already reported in previous study focusing on cyto-sine and methyl-cytosine electrooxidation in oligonucleotide environ-ment [29].

the opposite analytical response to their electrooxidation on the electrode surface, hindering their adsorption on the electrode due to size, steric and/or conformation impediments.

3.3.3. Identification of nucleobases in mixed synthetic solutions

According to Fig. 2, the electrochemical oxidation of C and U at the mbSPGE occurred at around +1.21 and +1.15 V vs. Ag/AgCl, respec- tively, making simultaneous identification of both nucleobases in a mixture almost impractical due to the proximity of the anodic peaks. By contrast, the electroanalytical response to the

$$C: j_{peak}\left(\mu A\Big/mm^2\right) = \frac{14.94\cdot C_i(mM)}{1 + 3.87\cdot C_i(mM)}; r^2 = 0.999 \qquad (5)$$

oxidation reaction of A and G was produced at +0.89 and +0.56 V vs. Ag/AgCl, respectively, enabling their qualitative discrimination. In this respect, the SWV response of a mixture of C, A and G in their unbrominated form was depicted in Figure S6. Comparing the single component response with the electrooxidation response of the multicomponent mixture, a shift of the SWV peaks associated with the nucleobases of about 50 mV toward a more positive potential was observed for each component. The latter was even more noticeable for C and G and possibly attributed to a matrix effect within the oxidation reaction. These results pointed out the

feasibility of qualitative electroanalytical detection of the three un- modified nucleobases, C, A, and G by their electrochemical oxidation upon mbSPGE. Furthermore, when U was added to the mixture, the

oxidation peaks associated with C and U overlapped in the range of +1.00 and +1.40 V vs. Ag/AgCl rendering the distinction between them troublesome (see Figure S6) as expected based on their individual response. Another point to be addressed was the evolution of the electrochemical response when both the non- and brominated nucleobases were present within the phosphate buffer solution, and whether it would still be possible to distinguish between the brominated nucleobase and its unmodified counterpart. In this regard, Fig. 5 shows the SWV response of different mixtures of BrU−U and BrC−C at mbSPGE. Different concentrations of the brominated molecule (from 0.5 to 1.5 mM) were studied by keeping the unmodified nucleic base constant at 2.5 mM. By comparing the SWV response of the mixture U and BrU, two well-defined anodic peaks were distinguished at ca. +1.16 and +0.99 V vs. Ag/AgCl, respectively, which allowed the identification of BrU in the presence of U. However, despite the U concentration was remained constant, its current density decreased upon increasing BrU concentration. Thus, the anodic peak attributed to U oxidation was strongly affected in the SWV profile by the presence of BrU, or even there was overlapping of the two anodic electrochemical signals.

As expected, based on how it behaves as a single component, BrU showed linear relationship between the peak current density and concentration following the equation: j_{peak} (μA/mm^2) = 0.337•C_{BrU} (mM) + 0.7993 (r^2 = 0.995). Nevertheless, the slope of the curve was reduced by four times compared to the slope found for the single component (Eq. (2)). Hence, this demonstrated the strong influence on the electrochemical response when both U and BrU coexist together. This fact might be attributed to a possible competition of electroactive site during the electrooxidation reaction undertaken.

In the case of the SWV response of the simultaneous presence of C and BrC (Fig. 5b), the detection of both nucleobases turned less evident due to the proximity of the oxidation potentials and foremost more significant was the shape of the peaks (wider than for U and BrU, Fig. 5a). This results in the overlap of the individual peaks observed in the manner of a broad hump between +0.90 and +1.35 V vs. Ag/AgCl. Nonetheless, taking advantage of this broad SWV response, it was possible to identify the brominated modification of cytosine undergone in the presence of C. With the aim to deeper analysis of the electroanalytic behaviour of this pair, the deconvolution of the broad peak into two contributions (Figure S7) allowed to obtain a relationship between current peak and BrC concentration following the equation: j_{peak} (μA/mm^2)= 0.979•C_{BrC} (mM) + 1.317 (r^2 = 0.999). The slope of the curve was twice lower than that obtained for the single component (Eq. (1)) confirming the high effect on the BrC electrochemical oxidation under the presence of its counterpart. Furthermore, it should be noted that the pairs A-BrA and G-BrG have not been examined as mixed solutions, since its individual oxidation potential (Fig. 2) allow to predict the high overlapping of the nucleobase and halogenated-nucleobase oxidation potential.

3.4. Simultaneous electrochemical behaviour of all three 5-halocytosines at mbSPGE

Once the behaviour of brominated nucleobases was analyzed, we turned out to study the effect of the halogen nature incorporated to the cytosine with the aim of expanding the study toward other halogens. Our previous work [19] showcased the qualitative detection of FC, ClC and BrC at GCE in 0.1 M acetate buffer pH 5, displaying SWV responses in the range of 1.27−1.31 V vs. Ag/AgCl. In this work, we went beyond GCE by employing mbSPGE under optimal conditions (0.1 M PBS pH 7.0) across these three halogenated cytosines. Fig. 6 depicts the SWV response of C and its halogenated nucleobases using the mbSPGE platform. The oxidation peaks were observed at +1.20, +1.02, +1.07 and +1.09 V vs. Ag/AgCl for C, FC, ClC and BrC, respectively. As seen, all the halocytosines showed well-defined peaks shifted towards lower potentials (ca. 150 mV) compared to C response. The anodic peaks were located close to each other with a slight trend toward more positive potential following BrC > ClC > FC. This is in concordance with Sanjuan
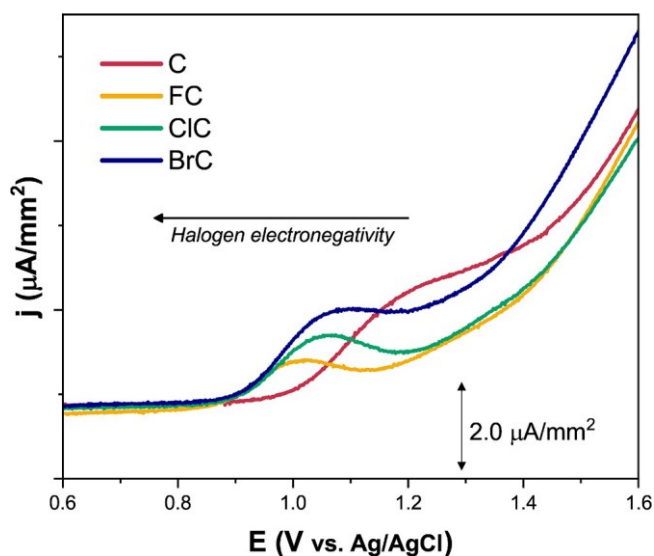

Fig. 6. Square wave voltammetry performed at mbSPGE for 0.6 mM of C, ClC, BrC and FC in 0.1 M PBS at pH 7.0. SWV parameters: pulse amplitude, 50 mV; potential step, 2 mV; frequency 4 Hz.
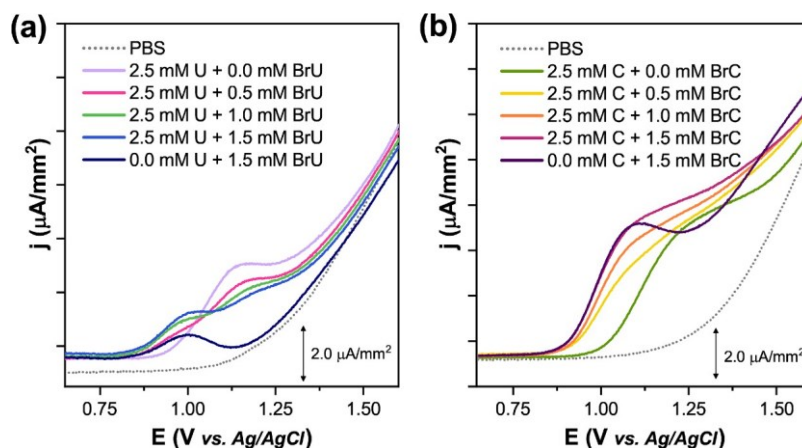

Fig. 5. Square wave voltammetry response of mixture of **(a)** U (2.5 mM), and BrU (from 0.5 to 1.5 mM) and **(b)** C (2.5 mM), and BrC (from 0.5 to 1.5 mM) in 0.1 M PBS at pH 7.0 at mbSPGE. SWV parameters: pulse amplitude, 50 mV; potential step, 2 mV; frequency 4 Hz.

et al. and was ascribed to the total free energy and solvation energy for the halogenated nucleobases.

Different concentrations of halogenated cytosines were tested in the range between 0.2 and 1.0 mM showing a linear response of peak current vs. concentration with r^2 = 0.993, 0.983, 0.990 and LOD of 0.139, 0.142, 0.110 mM for FC, ClC, and BrC, respectively. These results open up wide possibilities of electrochemical detection and quantification of different halogenations of C using screen-printed graphite electrodes at conditions that are close to physiological environment.

4. Conclusions

In this work, the electrochemical behaviour of different halogenated nucleobases on graphite screen-printed electrodes has been explored with the aim of demonstrating the qualitative detection of different epigenetic modifications on the nucleobases, namely bromination of G, A, U, and C. The results show the appearance of well-defined peaks related to the electrooxidation of the brominated nucleobases at physiological pH. The different electrochemical response, in terms of peak potential, peak shape and current density, could be attributed to changes in the electronic density within the nucleobase due to the effect of the Br atom, which has a significant influence on the interaction between the molecule and the carbon-based electrode surface. The results showed the higher current density obtained with the microband geometry as opposed to the planar disc- one working electrode, which is associated with the enhanced mass transport. Finally, a synthetic mixture of un-modified nucleobases, as well as a mixture of halogenated nucleobase and its counterpart, was analysed, revealing the possibility of detecting the bromination of some nucleobases, paving the way for research on the development of carbon-based point-of-care electrochemical sensors for epigenetic modification of RNA, directly related to the early diagnosis of several diseases.

References

[1] J.G. Lewis, D.O. Adams, Inflammation, oxidative DNA damage, and carcinogenesis, Environ. Health Perspect. 76 (1987) 19–27, https://doi.org/10.1289/EHP.877619.

[2] J.K. Kundu, Y.J. Surh, Emerging avenues linking inflammation and cancer, Free Radic. Biol. Med. 52 (9) (2012) 2013–2037, https://doi.org/10.1016/J.FREERADBIOMED.2012.02.035.

[3] V. Valinluck, L.C. Sowers, Inflammation-mediated cytosine damage: a mechanistic link between inflammation and the epigenetic alterations in human cancers, Cancer Res. 67 (12) (2007) 5583–5586, https://doi.org/10.1158/0008-5472.CAN-07-0846.

[4] I. Tischoff, C. Wittekind, A. Tannapfel, Role of epigenetic alterations in cholangiocarcinoma, J. Hepatobiliary. Pancreat. Surg. 13 (4) (2006) 274–279, https://doi.org/10.1007/S00534-005-1055-3/METRICS.

[5] T. Asahi, H. Kondo, M. Masuda, H. Nishino, Y. Aratani, Y. Naito, T. Yoshikawa, S. Hisaka, Y. Kato, T. Osawa, Chemical and Immunochemical Detection of 8-Halogenated Deoxyguanosines at Early Stage Inflammation, J. Biol. Chem. 285 (12) (2010) 9282–9291, https://doi.org/10.1074/JBC.M109.054213.

[6] K.S. Pandey, P.C. Mishra, Electronic spectra of 8-bromoguanine and 8-bromoadenine, J. Photochem. Photobiol. A Chem. 62 (1) (1991) 107–115, https://doi.org/10.1016/1010-6030(91)85109-T.

[7] A. Sassa, T. Ohta, T. Nohmi, M. Honma, M. Yasui, Mutational specificities of brominated DNA adducts catalyzed by human DNA polymerases, J. Mol. Biol. 406 (5) (2011) 679–686, https://doi.org/10.1016/J.JMB.2011.01.005.

[8] K. Shinmura, H. Kato, M. Goto, H. Tao, Y. Inoue, S. Nakamura, H. Yoshida, E. Tsuzaki, H. Sugimura, Mutation spectrum induced by 8-bromoguanine, a base damaged by reactive brominating species, in human cells, Oxid. Med. Cell Longev. (2017), https://doi.org/10.1155/2017/7308501.

[9] S. Vogel, K. Ebel, C. Heck, R.M. Schürmann, A.R. Milosavljević, A. Giuliani, I. Bald, Vacuum-UV induced DNA strand breaks – influence of the radiosensitizers 5-bromouracil and 8-bromoadenine, PCCP 21 (4) (2019) 1972–1979, https://doi.org/10.1039/C8CP06813E.

[10] L.F. Holroyd, T. Van Mourik, Stacking of the mutagenic base analogue 5-bromo-uracil: energy landscapes of pyrimidine dimers in gas phase and water, PCCP 17 (45) (2015) 30364–30370, https://doi.org/10.1039/C5CP04612B.

[11] W. Struck, M. Waszczuk-Jankowska, R. Kaliszan, M.J. Markuszewski, The state-of-the-art determination of urinary nucleosides using chromatographic techniques "hyphenated" with advanced bioinformatic methods, Anal. Bioanal. Chem. 401 (7) (2011) 2039–2050, https://doi.org/10.1007/S00216-011-4789-6/FIGURES/4.

[12] I. Honda, K. Itoh, M. Mizugaki, T. Sasaki, Creatinine at the Evaluation of Urinary 1-Methyladenosine and Pseudouridine Excretion, Tohoku J. Exp. Med. 188 (2) (1999) 133–138, https://doi.org/10.1620/TJEM.188.133.

[13] Y. Qing, Z. Tian, Y. Bi, Y. Wang, J. Long, C.X. Song, J. Diao, Quantitation and mapping of the epigenetic marker 5-hydroxymethylcytosine, Bioessays 39 (5) (2017) 1700010, https://doi.org/10.1002/BIES.201700010.

[14] Y. Wang, X. Hu, J. Long, J. Diao, Epigenetic optical sensing of 5-hydroxymethyl-cytosine at the single-molecule level, Sens. Actuators B Chem. 358 (2022) 131500, https://doi.org/10.1016/J.SNB.2022.131500.

[15] E. Povedano, V.R.V. Montiel, A. Valverde, F. Navarro-Villoslada, P. Yáñez-Sedeno, M. Pedrero, A. Montero-Calle, R. Barderas, A. Peláez-García, M. Mendiola, D. Hardisson, J. Feliú, J. Camps, E. Rodríguez-Tomàs, J. Joven, M. Arenas, S. Campuzano, J.M. Pingarrón, Versatile electroanalytical bioplatforms for simultaneous determination of cancer-related DNA 5-methyl- and 5-hydroxy-methyl-cytosines at global and gene-specific levels in human serum and tissues, ACS Sens. 4 (1) (2019) 227–234, https://doi.org/10.1021/ACSSENSORS.8B01339.

[16] Z. Xu, Z. Wang, D. Hu, H. Chen, Y. Yan, Y. Li, M. Tu, Q. Shen, X. Liu, R. Li, C. Lu, F. Xue, C. Xie, G. Yang, MXene boosted ultrasensitive electrochemical detection of 5-hydroxymethylcytosine in genomic DNA from complex backgrounds, Adv. Funct. Mater. 34 (19) (2024) 2313118, https://doi.org/10.1002/ADFM.202313118.

[17] S. Bilge, M.M. Gürbüz, S.A. Ozkan, B. Dogan Topal, Electrochemical sensor for the analysis of 5-hydroxymethylcytosine in the presence of cytosine using pencil graphite electrode, Anal. Biochem. (2024) 696, https://doi.org/10.1016/J.AB.2024.115674.

[18] M. Bartosik, L. Jirakova, Electrochemical analysis of nucleic acids as potential cancer biomarkers, Curr. Opin. Electrochem. 14 (2019) 96–103, https://doi.org/10.1016/J.COELEC.2019.01.002.

[19] I. Sanjuán, A.N. Martín-Gómez, J. Graham, N. Hernández-Ibáñez, C. Banks, T. Thiemann, J. Iniesta, The electrochemistry of 5-halocytosines at carbon based electrodes towards epigenetic sensing, Electrochim. Acta 282 (2018) 459–468, https://doi.org/10.1016/J.ELECTACTA.2018.06.050.

[20] R.L. Lundblad, F. Macdonald, Handbook of Biochemistry and Molecular Biology, CRC Press, Taylor & Francis Group, 2021. https://www.routledge.com/Handbook-of-Biochemistry-and-Molecular-Biology-Lundblad-Macdonald/p/book/9780367781132.

[21] J.P. Metters, R.O. Kadara, C.E. Banks, Electroanalytical properties of screen printed graphite microband electrodes, Sens. Actuators B Chem. 169 (2012) 136–143, https://doi.org/10.1016/J.SNB.2012.04.045.

[22] E.V. Suprun, G.R. Kutdusova, S.A. Khmeleva, S.P. Radko, Towards deeper understanding of DNA electrochemical oxidation on carbon electrodes, Electrochem. Commun. 124 (2021) 106947, https://doi.org/10.1016/j.elecom.2021.106947.

[23] J. Zhou, S. Li, M. Noroozifar, K. Kerman, Graphene oxide nanoribbons in chitosan for simultaneous electrochemical detection of guanine, adenine, thymine and cytosine, Biosensors 10 (2020) 30, https://doi.org/10.3390/bios10040030.

[24] A.M. Brett, F.M. Matysik, Voltammetric and sonovoltammetric studies on the oxidation of thymine and cytosine at a glassy carbon electrode, J. Electroanal.

Chem. 429 (1–2) (1997) 95–99, https://doi.org/10.1016/S0022-0728(96)05018-8.

[25] Wang, H.S., Ju, H.X., Chen, H.Y. (2002). Simultaneous determination of guanine and adenine in DNA using an electrochemically pretreated glassy carbon electrode https://doi.org/10.1016/S0003-2670(02)00297-0.

[26] S. Steenken, S.V. Jovanovic, How easily oxidizable is DNA? One-electron reduction potential of adenosine and guanosine radicals in aqueous solution, J. Am. Chem. Soc. 119 (1997) 617–618, https://doi.org/10.1021/ja962255b.

[27] C.M.C. Andres, J.M. Pe´rez de la Lastra, C.A. Juan, F.J. Plou, E. Pe´rez-Leben˜a, Chemical insights into oxidative and nitrative modifications of DNA, Int. J. Mol. Sci. 24 (2023) 15240, https://doi.org/10.3390/ijms242015240.

[28] A.M. Brett, J.A.P. Piedade, L.A. Silva, V.C. Diculescu, Voltammetric determination of all DNA nucleotides, Anal. Biochem. 332 (2) (2004) 321–329, https://doi.org/10.1016/J.AB.2004.06.021.

[29] A. Brotons, L.A. Mas, J.P. Metters, C.E. Banks, J. Iniesta, Voltammetric behaviour of free DNA bases, methylcytosine and oligonucleotides at disposable screen printed graphite electrode platforms, Analyst 138 (18) (2013) 5239–5249, https://doi.org/10.1039/C3AN00682D.

[30] R.G. Compton, G.G. Wildgoose, N.V. Rees, I. Streeter, R. Baron, Design, fabrication, characterisation and application of nanoelectrode arrays, Chem. Phys. Lett. 459 (1– 6) (2008) 1–17, https://doi.org/10.1016/J.CPLETT.2008.03.095.

[31] Inzelt, G. (2002). Electroanalytical Methods: guide to experiments and applications. In F. Scholz (Ed.), The Chemical Educator 2002 7:5 (2nd ed., Vol. 7, Issue 5). Springer. https://doi.org/10.1007/S00897020608A.

[32] F. Martínez-Rojas, M.A. Del Valle, M. Isaacs, G. Ramírez, F. Armijo, Electrochemical behaviour study and determination of guanine, 6-thioguanine, acyclovir and gancyclovir on fluorine-doped SnO2 electrode, application in pharmaceutical preparations, Electroanalysis 29 (12) (2017) 2888–2895, https://doi.org/10.1002/ELAN.201700516.

[33] I. Langmuir, The adsorption of gases on plane surfaces of glass, mica and platinum, J. Am. Chem. Soc. 40 (9) (1918) 1361–1403, https://doi.org/10.1021/JA02242A004/ASSET/JA02242A004.FP.PNG_V03.